Earth Surf. Dynam. Discuss., https://doi.org/10.5194/esurf-2017-64
Manuscript under review for journal Earth Surf. Dynam.
Discussion started: 20 November 2017

On the Holocene Evolution of the Ayeyawady Megadelta

Authors:

Liviu Giosan[1], Thet Naing[2], Myo Min Tun[3], Peter D. Clift[4], Florin Filip[5], Stefan Constantinescu[6], Nitesh Khonde[1,7], Jerzy Blusztajn[1], Jan-Pieter Buylaert[8], Thomas Stevens[9], Swe Thwin[10]

Affiliations:

[1]Geology & Geophysics, Woods Hole Oceanographic, Woods Hole, USA
[2]Pathein University, Pathein, Myanmar
[3]University of Mandalay, Mandalay, Myanmar
[4]Geology & Geophysics, Louisiana State University, USA
[5]The Institute for Fluvial and Marine Systems, Bucharest, Romania
[6]Geography Department, Bucharest University, Bucharest, Romania
[7]Birbal Sahni Institute of Palaeosciences, Lucknow, India
[8]Technical University of Denmark, Roskilde, Denmark
[9]Uppsala University, Uppsala, Sweden
[10]Mawlamyine University, Mawlamyine, Myanmar

Correspondence to: L. Giosan (lgiosan@whoi.edu)

Earth Surf. Dynam. Discuss., https://doi.org/10.5194/esurf-2017-64
Manuscript under review for journal Earth Surf. Dynam.
Discussion started: 20 November 2017

Abstract:

The Ayeyawady delta is the last Asian megadelta whose evolution has remained essentially unexplored so far. Unlike most other deltas across the world, the Ayeyawady has not yet been affected by dam construction providing a unique view on largely natural deltaic processes benefiting from abundant sediment loads affected by tectonics and monsoon hydroclimate. To alleviate the information gap and provide a baseline for future work, here we provide a first model for the Holocene development of this megadelta based on radiocarbon and optically stimulated luminescence-dated trench and drill core sediments collected in 2016 and 2017, together with a re-evaluation of published maps, charts and scientific literature. Altogether, this data indicates that Ayeyawady is a mud-dominated delta with tidal and wave influences that has been constructed within a vertically stable Pleistocene incised valley. The sediment-rich Ayeyawady River built meander belt alluvial ridges with avulsive characters. A more advanced coast in the western half of delta (i.e., the Pathein lobe) was probably favored by the more western location of the early course of the river. Radiogenic fingerprinting of the sediment suggest that the Pathein lobe has been built with Ayeyawady sediments alone. However, the eastern region of the delta (i.e., Yangon lobe) is offset inland and extends east into the mudflats of the Sittaung estuary. Wave-built beach ridge construction during the late Holocene, similar to other several deltas across the Indian monsoon domain, suggests a common climatic control on monsoonal delta morphodynamics through variability in discharge, changes in wave climate, or both. Correlation of the delta morphological and stratigraphic architecture information onland to the shelf bathymetry as well as its tectonic, sedimentary and hydrodynamic characteristics provide insight on the peculiar growth style of the Ayeyawady delta. The offset between the western Pathein lobe and the eastern deltaic coast appears to be driven by tectonic-hydrodynamic feedbacks as the extensionally lowered shelf block of the Gulf of Mottama amplifies tidal currents relative to the western part of the shelf. This situation probably activates a perennial shear front between the two regions that acts as a leaky energy fence helping to trap part of the sediment within the Pathein shore-attached subaquoeus clinoform. Just as importantly, the strong currents in the Gulf of Mottama act as an offshore-directed tidal pump that help build the deep mid-shelf Mottama clinoform with mixed sediments from Ayeyawady, Sittaung, and Thanlwin rivers. The highly energetic tidal, wind and wave regime of the northern Andaman Sea thus exports most sediment offshore despite the large load of the Ayeyawady river. The expected sediment deficit if dams are constructed on the river and tributaries may significantly impact the Ayeyawady delta fragile sedimentary equilibrium making it more vulnerable to the accelerating sea level rise and changes in frequency and intensity of cyclones hitting the coast.

Earth Surf. Dynam. Discuss., https://doi.org/10.5194/esurf-2017-64
Manuscript under review for journal Earth Surf. Dynam.
Discussion started: 20 November 2017

77 Introduction
78
79 Asian megadeltas (*Woodroffe et al., 2006*) have a long history of human habitation and
80 anthropogenic impact. With large populations, which increasingly coagulate in sprawling
81 megacities, these vast low-lying and ecologically-rich regions are under threat from
82 environmental degradation, climate change and sea level rise. The Ayeyawady (formerly
83 known as Irrawaddy) is the least studied of these megadeltas despite its scientific, social
84 and economical importance (*Hedley et al., 2010*). Located in the larger India-Asia
85 collision zone, the Ayeyawady delta (Fig. 1) bears the imprint of uniquely complex
86 tectonic processes in a region of oblique subduction (*Morley et al., 2017*) and is a
87 repository for unusually large sediment yields under an erosion-prone monsoon climate
88 (e.g., *Giosan et al., 2017*). Sediment redistribution within the delta and on the shelf
89 fronting it is affected by strong tides amplified by the geomorphology of the region
90 (*Ramasawamy and Rao, 2014*). In contrast to other Asian megadeltas, the Ayeyawady
91 river basin is arguably less transformed by post-World War II anthropogenic impacts
92 although humans have probably affected delta development since at least the Iron Age as
93 agriculture expanded along the river (*Moore, 2007*) and later intensified during the Pyu,
94 Bagan, and Ava historical periods. Recent rapid development trends and population
95 growth underline the need to understand the history and document the current state of the
96 Ayeyawady delta.
97
98 Although the Ayeyawady River is less regulated compared to other large rivers, plans are
99 afoot to construct several dams across it and this may change the water and sediment
100 regimes, as well as fluxes reaching its low-lying delta plain (*Brakenridge et al., 2017*).
101 Inundation of the Ayeyawady delta region during cyclone Nargis in 2008 was one of the
102 costliest and deadliest natural disasters ever recorded (*Fritz et al., 2009; Seekins, 2009*).
103 Catastrophic monsoon-driven river floods are also common and devastating (*Brakenridge*
104 *et al., 2017*). The Ayeyawady delta may already be sediment deficient (*Hedley et al.,*
105 *2010*) and the anticipated sediment deficit after damming could increase its vulnerability
106 to such transient events as well as to long term sea level rise (*Giosan et al., 2014*). Strong
107 tidal currents in the northern Andaman Sea (*Rizal et al., 2012*) amplify some aspects of
108 delta vulnerability, such as salinization (*Taft and Evers, 2016*) whereas other aspects may
109 be attenuated such as sediment redistribution along the coast or sediment trapping within
110 the subaerial delta (e.g., *Hoitink et al., 2017*). Better knowledge on how the delta has
111 formed and functioned will help future efforts to maintain it viable.
112
113 To alleviate the information gap and provide a baseline for future work we sketch here a
114 first model for the Holocene evolution of the Ayeyawady delta based on new field data
115 collected in two expeditions in 2016 and 2017 (Figs. 2 and 3; see Fig. S1 for site
116 locations and names) together with a re-evaluation of published maps, charts and
117 scientific literature (Fig. 4 and 5). In the process we reassess our knowledge concerning

monsoonal deltas in general by advancing new ideas on how morphodynamics and sedimentary architecture can be controlled by feedbacks between tectonics and tides as well as by the balance between fluvial discharge and wave climate.

Background

The Ayeyawady River is a major fluvial system that became individualized in Oligocene/Early Miocene (Fig. 1; *Morley, 2017* and references therein). The upper Cretaceous subduction of the Neotethys Ocean followed by the collision between India and Asia led to the uplift of the Indo-Burman Ranges accretionary prism and foreland basin sediments extending southward as far as the Andaman Islands (*Racey and Ridd, 2015*). The Central Myanmar Basin (CMB) was isolated in the process from the Bay of Bengal. The complex of basins forming the CMB include the Ayeyawady Valley separated by the Bago Yoma (Pegu Yoma) from the Sittaung (Sittang) Valley flowing along the Shan Plateau. The Ayeyawady River infilled this ~900 km long shallow marine area toward the Andaman Sea, a Cenozoic backarc/strike-slip basin induced by oblique subduction of the Indian plate under Eurasia (e.g., *Curray, 2005*). A southern shift in Ayeyawady deposition was evident in the Miocene after the strike-slip Sagaing Fault activated along Bago Yoma. The Holocene delta is the last realization in a series of deltas comprising this southward-moving Ayeyawady depocenter.

Myanmar's hydroclimate that is responsible for Ayeyawady flow is spatially complex owing to its varied topography and compound influences from both the Indian and East Asian monsoon systems (*Brakenridge et al., 2017*). Orographic precipitation occurs along the northeastern Himalayas and Indo-Buman Ranges (*Xie et al., 2006*), as well as the Shan Plateau feeding the upper Ayeyawady and the Chindwin, whereas Central Myanmar, in the lee of these ranges, remains drier. The upper basin of the Ayeyawady also receives snow and glacier meltwater in the spring. Over 90% of the discharge at the delta occurs between May and October with small but significant interannual variability (*Furuichi et al., 2009*) linked to the El Nino-Southern Oscillation, Indian Ocean Dipole, and Pacific Decadal Oscillation (*D'Arigo and Ummenhofer, 2014* and references therein).

In historical times the Ayeyawady River has transported ~422 ± 41 × 10^9 m^3 of freshwater every year to the ocean (*Robinson et al, 2007*), watering Myanmar from north to south along the way (Fig. 1). The water discharge apparently decreased to the present level of 379 ± 47 × 10^9 m^3/year (*Furuichi et al., 2009*). Among the delta-building Himalayan rivers, the Ayeyawady is a prodigious sediment conveyor (~364 ± 60 × 10^6 t/year), second only to the combined Ganges-Brahmaputra (*Robinson et al, 2007*). Between 40 and 50 % of the sediment comes from the upper Ayeyawady with the rest supplied by its main tributary, the Chindwin (*Garzanti et al., 2016*). Sediments

158 transported by the Upper Ayeyawady River come primarily from erosion of gneisses and
159 granitoids of the Himalayan Eastern Syntaxis region and the Sino-Burman Ranges.
160 Although draining less steep terrain, the Chindwin contributes more sediment than the
161 Upper Ayeyawady from the easily erodible flysch and low-grade metasedimentary rocks
162 of the Indo-Burman Ranges. Both water and sediment discharge vary in sync at
163 interannual time scales as a function of monsoon intensity (*Furuichi et al., 2009*), but
164 they changed little since the late 19th century when *Gordon (1893)* measured them
165 systematically for the first time. In addition to the Ayeyawady, the Sittaung River
166 supplies sediment to the northern shore of the Gulf of Mottama (*aka* Gulf of Martaban)
167 where its estuary merges with the Ayeyawady delta coast (Fig. 1). The sediment
168 discharge from the Sittaung is unknown but can be estimated based on its annual water
169 discharge range from 50×10^9 m^3 to a maximum of 40 to 50×10^6 t/year by assuming
170 sediment yields similar to the Ayeyawady (*Milliman and Farnsworth, 2010*). Another
171 sediment contributor to the Gulf of Mottama (~180×10^6 t/year; *Robinson et al, 2007*) is
172 the Thanlwin River (Salween) draining the eastern Shan Plateau and eastern Tibetan
173 Plateau. Information about the variability in Ayeyawady's sediment discharge over the
174 Holocene lifetime of the delta is sparse, as are reconstructions for the monsoon regime in
175 its basin. Assuming the modern direct correlation between water discharge and sediment
176 load one may qualitatively infer an increase in sediment delivery since 10,000 years ago
177 with a peak in around 5000 years ago when the Andaman Sea was at its freshest
178 (*Gebregeorgis et al., 2016*), followed by a decrease to the present values, as the Indian
179 monsoon has weakened since the Early Holocene (e.g., *Ponton et al., 2012*).
180
181 The Ayeyawady delta is a mud-dominated delta that exhibits mainly tidal and secondarily
182 wave influences (Figs. 2 and 5; *Kravtsova et al., 2009*). Ayeyawady's single braided
183 channel starts to show avulsive behaviour near the town of Myan Aung (~18.2°N) where
184 the tidal influence is still felt ~290 km from the Andaman Sea (Fig. 1). The apex of the
185 delta, defined as the region of deltaic distributary bifurcation, is north of the town of
186 Hinthada (18°N) around 270 km from the coast. Multiple branches are active in the delta,
187 splitting and rejoining to form a network of lower order distributary channels and
188 reaching the coast through eleven tidally-enlarged estuaries (Fig. 2). Most of the water
189 discharge (76%) is delivered to the Andaman Sea through three main mouths: Pyamalaw,
190 Ayeyawady and To-Thakutpin from west to east (*Kravtsova et al., 2009*).
191
192 In natural conditions when the delta was covered by tropical forests and mangroves
193 (*Adas, 2011*), sedimentation on the delta plain occurred within active and abandoned
194 channels, on channel levees and inter-distributary basins (*Stamp, 1940; Kravtsova et al.,*
195 *2009*). The coast prograded via shoal/bar emergence and wave-built beach ridges with
196 associated interridge swales (*Kravtsova et al., 2009*). The coastline for the Ayeyawady
197 delta proper stretches from the western rocky Cape Maw Deng, adjacent to the Pathein

River, to the Yangon River in the east (Fig. 1). However, this conventional definition does not capture the fact that the accumulative coast with sediment input from the Ayeyawady continues east of Yangon River into the Sittaung estuary. Despite the large fluvial sediment load of the combined Ayeyawady and Sittaung delivered annually (350–480 × 10^6 t), shoreline changes have been puzzlingly minor along the Ayeyawady delta coast since 1850 (*Hedley et al., 2010*). Sea level change data is sparse and unreliable for the delta and no data on subsidence/uplift exists.

The shelf morphology in front of the Ayeyawady delta is complex due to its tectonic structure and the nature of Holocene sedimentation (*Rodolfo, 1969a,b, 1975; Ramaswamy and Rao, 2014*). The width of the shelf is ~170 km wide off the Ayeyawady River mouths, widening to more than 250 km in the Gulf of Mottama (otherwise known as the Gulf of Martaban; Figs. 1 and 5). The shelf edge exhibits a flat, platform-like indentation in the Gulf of Mottama between 140 and 180 m deep (i.e., the Martaban Depression - *Ramaswamy and Rao,* 2014) that features a poorly defined dendritic network of channels feeding the Martaban Canyon (*Rodolfo, 1975)*. Most of the large Ayeyawady sediment load is redistributed by the strong tidal currents (Fig. 5) and deposited on the wide northern Andaman shelf (*Ramaswamy and Rao, 2014*) where it mixes with sediment from the Sittaung, Thanlwin and other smaller rivers (*Damodararao et al., 2016*). Semi-diurnal tides vary between 2 and 3 m from the Pathein River to the Bogale River reaching higher stages inside distributaries. The tidal range is gradually amplified to macrotidal conditions on the shallow (<30 m) shelf of the Gulf of Mottama from the Bogale Promontory toward the Sittaung estuary where it reaches above 7 m during spring tides (*British Admiralty, 1935*). Associated tidal currents also vary accordingly to over 3.5 m/s near the Sittaung mouth.

Waves are subordinate in importance to tides, with average heights less than 1 m in winter to 1–2 m in summer (*Kravtsova et al., 2009*). Tidal currents combine with the wind-driven circulation. Wind currents are clockwise during the summer monsoon and reversed during the winter monsoon (*Rizal et al., 2012*). The macrotidal regime maintains turbid conditions year-round with the turbidity front oscillating ~150 km in the Gulf of Mottama in phase with the spring-neap tidal cycle (*Ramaswamy et al. 2004*). Annual turbidity levels and suspended sediment distribution are modulated by the monsoonal-driven winds, currents and river discharge (*Ramaswamy et al. 2004; Matamin et al, 2015*) with the most extensive and compact turbid waters occurring in boreal winter. During the summer the turbidity region shrinks to the Gulf of Mottama and nearshore regions where river plumes are active and dispersed eastward. Turbidity profiles show an increase with depth during fair-weather and uniform concentrations during major storms or cyclones (*Ramaswamy et al. 2004; Shi and Wang 2008*). Bottom nepheloid layers and

possibly hyperpycnal flows occur in the Gulf of Mottama and flow into the interior of the Andaman Sea as mid-water nepheloid layers (*Ramaswamy et al. 2004*).

The bathymetric characteristics of the shelf and the circulation system favor deposition of fluvial sediments in a mudbelt that widens from western edge of the Ayeyawady coast into the Gulf of Mottama that more or less coincides in extent with the high turbidity region (*Ramaswamy and Rao, 2014*). The outer shelf, including the Martaban Depression, is a zone of low to non-deposition, and exhibits a relict morphology with topographic irregularities that host relict coarse-grained carbonate-rich sediment and fauna with patchy Holocene muds (*Ramaswamy and Rao, 2014*).

In terms of human impacts on the delta it is important to note that the population of Myanmar increased from 4–5 million in the late 19th century to ~51 million in 2014 with 30% residing in the Ayeyawady delta region. This large increase in population led to a rapid rate of deforestation in the basin, but also to destruction of mangroves for agriculture and fuel in the delta (*Taft and Evers, 2016*). An earlier large migration wave to the delta occurred in the latter half of the 19th century when the British colonial authorities cleared much of the delta forests and mangroves for rice agriculture (*Adas, 2011*). Construction of dikes to protect agricultural lands in the delta began in 1861 and continued aggressively until the 1920s. These dikes are generally of a horseshoe type protecting delta islands in the upstream and sides from the floodwave but recently poldering with diking entire islands was employed. Most channels remain natural with no extensive system of dredged canals. However, all dikes limit overbank flooding and deposition of sediment (*Volker 1966; Stamp 1940*) and the entire agricultural system favors salinization of soils in the delta. The model for the Holocene evolution of the Ayeyawady delta that we provide below allows us to assess first order relationships to the complex regional tectonics, climate, and shelf circulation as a baseline for the future development and management of the delta.

Methods

The large scale morphology of the Ayeyawady delta, together with the adjoining regions (Fig. 2), were assessed and studied using satellite data and old maps of the region. High-resolution (90-m) digital elevation data were derived from NASA's Shuttle Radar Topography Mission (SRTM; *Farr et al., 2007*). Digital elevation models (DEMs) were constructed at 300 m resolution and were used in combination with Advanced Spaceborne Thermal Emission and Reflection Radiometer (ASTER) and Google Earth to identify geomorphic features that provide insight into fluvial morphodynamics. The delta and upstream floodplain was delimited from adjacent hinterlands with associated marginal alluvial fans as were remnant inselberg-like pre-deltaic terrains inside the delta. We identified active and abandoned river courses and delta distributaries and their

meandering belts. Finally, we identified fossil beach ridges denoting former delta shorelines. Guided by this assessment, in two field expeditions in the Ayeyawady delta in 2016 and 2017, we collected sedimentary records from shallow hand-dug trenches and cores with mechanized pneumatic and percussion drilling (Figs. 2 and 3; see also Fig. S1).

Fossil wave-built beach ridges were targeted by trenching in order to obtain a chronology for the delta coast advance (Figs. 1 and 2; see also Fig. S1). Samples for Optically Stimulated Luminescence (OSL) dating were collected where possible from within the beach-foreshore facies in water tight opaque tubes (site I-11 at Labutta in the western side of the delta; sites I-12 and I-13 at Seikma near the central delta coast; and site I-14 at Kungyangon near the eastern delta coast). A sample was collected in the anthropogenic overburden to date habitation on a Labutta beach ridge (Site I-10). In addition, two levee samples were collected on the youngest and one of the oldest meanders of the now defunct western major branch of the Ayeyawady (Figs. 1 and 2; Table 2) near the apex of the delta (sites I-8 near Ta Loke Htaw and I-9 near Lemyethna).

Drill coring was designed to recover continuous sediment records to the pre-deltaic Pleistocene sediments (Figs. 2 and 3; see also Fig. S1; Table 1). Drill sites were located in the middle and near the apex of the delta (core IR1 to 70.4 m depth at Kyonmangay located 6.7 m above sea level and core IR2 to 43 m depth at Ta Loke Htaw located at 18 m above sea level, respectively) to assess the deltaic architecture and, in particular, how far the post-glacial transgression reached inside the suspected Pleistocene Ayeyawady incised valley. Facies analysis was based on the visual description of lithology, sedimentary structures, textures and benthic foraminifera presence. In addition, XRF-scanning high resolution chemostratigraphy was employed for the drill cores to identify depositional environments using Woods Hole Oceanographic Institution's (WHOI) ITRAX XRF scanner (see methodology in *Croudace et al., 2006*). From the suite of measured elements we used [Si]/[Rb] ratio to characterize the sand content (i.e., Si-rich sand relative to fine grained muds, rich in Rb; *Croudace and Rothwell, 2015*), the [Br]/[total XRF counts] ratio or Br* to characterize the organic matter (i.e., with Br enriched in marine organic matter; *McHugh et al., 2008*), and [S]/[Rb] ratio to characterize redox conditions in fine-grained muds (i.e., with S in excess of terrigenous values in reducing conditions; *Croudace and Rothwell, 2015*).

Sediment sources for the pre-modern delta were estimated using radiogenic isotopes (Nd and Sr) on a bulk sediment sample from the delta apex trench (I-8 taken as representative for Ayeyawady fluvial sediment). To assess any potential addition of non-Ayeyawady sediment sources (e.g., littoral drift, marine biogenic carbonates) another pre-modern sample from the youngest dated fossil beach ridge trench near the coast (I-12) was

Earth Surf. Dynam. Discuss., https://doi.org/10.5194/esurf-2017-64
Manuscript under review for journal Earth Surf. Dynam.
Discussion started: 20 November 2017

318 measured both as bulk and decarbonated. Nd and Sr chemistry was undertaken with
319 conventional ion chromatography following the method of *Bayon et al. (2002)*. Strontium
320 was separated and purified from samples using Sr-Spec (Eichrom) resin. Nd chemistry
321 was performed with LN resin (Eichrom) following method described in *Scher and*
322 *Delaney (2010)*. Sr and Nd analyses were conducted on the NEPTUNE multi-collector
323 ICP-MS at WHOI with the internal precision around 10–20 ppm (2σ); external precision,
324 after adjusting $^{87}Sr/^{86}Sr$ and $^{143}Nd/^{144}Nd$ values by 0.710240 and 0.511847 for the
325 SRM987 and La Jolla Nd standards respectively, is estimated to be 15–25 ppm
326 (2σ).$^{143}Nd/^{144}Nd$ isotopic composition is expressed further as εNd (*DePaolo and*
327 *Wasserburg, 1976*) units relative to ($^{143}Nd/^{144}Nd$)CHUR= 0.512638 (*Hamilton et al.,*
328 *1983*).
329
330 Plant and wood pieces were radiocarbon-dated to derive a chronology for the deltaic
331 sediment succession and the pre-deltaic base (Table 1). Accelerator mass spectrometry
332 (AMS) radiocarbon dating was performed at the National Ocean Sciences Accelerator
333 Mass Spectrometry Facility (NOSAMS) at the WHOI. The methodology for AMS
334 radiocarbon dating is presented on the NOSAMS site (www.whoi.edu/nosams) and
335 discussed in *McNichol et al. (1995)*. All dates have been converted to calendar ages using
336 CalPal 4.3 (*Bronk Ramsey, 2009*) and the IntCal13 calibration dataset (*Reimer et al.,*
337 *2013*).
338
339 Seven samples were collected for OSL dating. Samples were collected using light-tight
340 metal tubes hammered horizontally into cleaned sediment surfaces. The tubes were
341 opened under subdued orange light at the Nordic Laboratory for Luminescence Dating
342 (Aarhus University) located at Risø (DTU Nutech) in Denmark. Using standard sample
343 preparation techniques (wet sieving, acid treatment, heavy liquids) purified quartz and K-
344 feldspar-rich extracts in the 180-250 µm grain size range were obtained (except sample
345 177202 for which it was 90-180 µm). Multi-grain aliquots of quartz and K-feldspar were
346 measured using a SAR protocol (*Murray and Wintle, 2000*) suitable for young samples.
347 The purity of the quartz OSL signal was confirmed using OSL IR depletion ratio test
348 (*Duller, 2003*; all aliquots within 10% of unity). For quartz OSL preheating for dose and
349 test dose was 200°C/10s and 160°C, respectively and K-feldspar rich extracts were
350 measured using a post-infrared (IR) Infrared Stimulated Luminescence (IRSL)
351 (pIRIR150) protocol based on *Madsen et al.* (2011). Early and late background
352 subtraction was used for quartz OSL and feldspar pIRIR dose calculations respectively.
353 Total dose rates to quartz and K-feldspar were calculated from radionuclide
354 concentrations measured on the outer material from the tubes using high resolution
355 gamma ray spectrometry (*Murray et al., 1987*). Samples were assumed to have been
356 saturated with water throughout the entire burial lifetime.
357

The morphology of the subaqueous extension of the Ayeyawady delta was studied using the only available detailed bathymetric chart of the region that was based on surveys from 1850 to 1929 with small corrections until 1935 (*British Admiralty, 1935*). Newer navigation charts of the region report only small corrections afterwards. The final DEM (Figs. 4 and 5) consists of 6442 individual soundings reduced to the original datum at Elephant Point at the entrance in Yangon River; to these we added the digitized bathymetric contours of the original chart. To extend the bathymetry offshore beyond the coverage of the original chart we used GEBCO 2014 Grid (General Bathymetric Charts of the Oceans, a global 30 arc-second interval grid). Prior to digitizing, all charts and satellite photos used in this study were georeferenced and transformed to a common UTM projection (Zone 46 N) with Global Mapper 18.0 (http:// www.globalmapper.com/) using 16 control points for each chart or photo. DEMs at a 250 m spatial resolution were generated from digitized soundings with Surfer 12.0 software (Golden Software, Inc.). The ‘‘natural neighbor’’ algorithm was chosen for interpolation because it is suitable for a variable density of data across the interpolation domain and does not extrapolate depth values beyond the range of existing data.

Results

In concert with satellite photos, our SRTM digital elevation model (Fig. 2a) reveals that the morphologically-defined Ayeyawady delta plain starts immediately after the river emerges from its mountainous valley at Myan Aung, bound on the western side by the Indo-Burma Range and massive alluvial fans originating in the Bago Yoma on the eastern side. Several inselberg-like pre-deltaic high terrains occur close to the coast on the western side of Pathein River and on both sides of Yangon River. Two alluvial ridges, 5 to 7 m high relative to their adjacent delta plain, with visible meander belts and rare crevasse splays, were constructed by large trunk channels (Fig. 2a, b, c). The western alluvial ridge along the Daga course is largely fossil, whereas the eastern ridge is being built along the present course of the river (Fig. 2c). Both ridges taper off in the mid-delta as the trunk channels start to bifurcate into distributaries that split and rejoin on the outer delta (Fig. 2a,b). After the bifurcation zone the delta plain is uniformly low in altitude (<5 m) with the exception of the higher mudflats near the entrance in the Sittaung estuary (Fig. 2a). Although possessing meander belts of their own in their upper reaches, the Pathein and Yangon Rivers, located at the western and eastern edge of the delta, do not show visibly large alluvial ridges (Fig. 2a, b) suggesting that they were not preferential routes for the main trunk Ayeyawady but secondary courses. Near the coast, several generations of wave-built beach ridges are evident in the outer part of the delta, bundling occasionally into beach ridge plains on the Bogale Promontory and on the sides on Yangon River (Fig. 2b).

Earth Surf. Dynam. Discuss., https://doi.org/10.5194/esurf-2017-64
Manuscript under review for journal Earth Surf. Dynam.
Discussion started: 20 November 2017

Sediment in our trenches on the Ayeyawady beach ridges exhibited weakly stratified, mud-rich, fine sand lithologies. The IR1 drill core (Fig. 3) at Kyonmangay (Fig. 2; see also Fig. S1) shows a succession of delta plain bioturbated soils and delta plain muds overlaying amalgamated fine to medium sand and muds of the delta front and prodelta/estuarine clayey muds with intercalated organic-rich detritus layers. Marine influences are documented in the prodelta/estuarine and delta front deposits by high Br* and rare benthic foraminifers. Tidal influence is indicated by thick-thin and sand-mud alternations in the delta front deposits. Flooding is suggested by occasional clean sandy layers in the prodelta facies. Both the delta plain and prodelta/estuarine deposits show increased S/Rb values indicating poorly oxic conditions. The transition to delta front advance at Kyonmangay occurred at 13.5 m below sea level (mbsl) ~8,100 years ago, as documented by the radiocarbon content of a leaf fragment. The deltaic succession stands on a 9,300 years old mangrove basal peat at 28.5 mbsl that tops thin weakly laminated mudflat deposits. Pre-Holocene fluvial deposits older than 10,200 years BP occur below, consisting of structureless medium to coarse sands with clayey mud intercalations, gravels, and fine-grained weakly laminated channel infills.

The IR2 drill core (Fig. 3) at Ta Loke Htaw (Fig. 2; see also Fig. S1) near the delta apex on the modern alluvial ridge exhibits a succession of delta plain sandy muds topping structureless medium sands with rare intercalated thin muds of channel/point bar type. They overlie fine-grained, weakly laminated channel infill deposits and floodplain fine sands with intercalated thin muds that started to accumulate ~8,900 years BP (radiocarbon dated wood piece). Below ~25 mbsl structureless fine to medium sands of channel/point bar and gravel layers occur to the base of the drill core. Organic material is rare in all facies at Ta Loke Htaw except for occasional wood branches and a tree trunk in the upper point bar facies. Marine influence is absent as foraminifers are not encountered and Br* levels are consistently low.

The quartz OSL and feldspar pIRIR150 luminescence dating results are summarized in Table 2 and Table S1. The quartz OSL signal is dominated by the fast component and the average dose recovery ratio is 1.00±0.02 (4 samples, 11-12 aliquots per sample) suggesting that our quartz De values measured using SAR are reliable. One prerequisite for accurate age estimation is that the quartz OSL signal was sufficiently bleached prior to burial in the sediment sequence. In this study we use the feldspar IR50 and pIRIR150 age data to provide insights into the completeness of bleaching of the quartz OSL signal (e.g., *Murray et al., 2012; Rémillard et al., 2016*). This is based on the observation that feldspar signals bleach much more slowly than quartz OSL (*Godfrey-Smith et al., 1988; Thomsen et al., 2008*): IR50 signals bleach approximately one order of magnitude slower than quartz OSL and pIRIR signals bleach even more slowly than IR50 signals (e.g., *Kars et al., 2014; Colarossi et al., 2015*). We are confident that the quartz signal is well-

bleached when the pIRIR150 age agrees within uncertainty with the quartz age; this is the case for sample 177204. We consider that the quartz OSL signal is very likely to be completely bleached when the IR50 age agrees or is slightly lower (due to fading) than the quartz age. This is the case for all samples except for sample 177202 for which the IR50 age may be slightly older. Nevertheless, this does not mean the quartz OSL age for this particular sample is affected by partial bleaching; we just cannot be certain it is not.

Overall, optical ages on the natural levee of one of the oldest meander series of the fossil eastern alluvial ridge indicate that the Daga course was active ~1,750±320 years ago, or possibly younger if the sample (177202 in Table 2) was partially bleached, whereas the natural levee on the youngest meander stopped growing ~1,500±230 years ago (Fig. 2; see also Fig. S1). This abandonment of the Daga and the avulsion to the present Ayeyawady course is also constrained by a radiocarbon date calibrated to ~1,300 years ago on a large wood trunk from the point bar facies drilled at Ta Loke Htaw. Based on our combined chronology the Ayeyawady delta reached as far south as the latitude of the cities of Yangon and Pathein around 6,300 years ago, as documented by a radiocarbon content of a leaf fragment from the delta plain facies at Kyonmangay. Optical dating shows that the least advanced beach ridge bundle found on the western side of the delta near Labutta is also the oldest (~4,600 years old; Fig. 2 and Fig. S1). The beach ridge plain at the Bogale Promontory started ~1,000 years ago, soon after beach ridges started to form at the Yangon River mouth (~1,200 years ago; Fig. 2 and Fig. S1).

Radiogenic provenance fingerprinting of the bulk river sediment on the Ta Loke Htaw levee shows that $^{143}Nd/^{144}Nd$ (εNd) and $^{87}Sr/^{86}Sr$ values of 0.512263 (-7.3) and 0.7120 respectively, close to the beach ridge sediment composition: 0.512285 (-6.9) and 0.7118 for bulk sediment and 0.512287 (-6.8) and 0.7119 for bulk decarbonated sediment. The identical $^{87}Sr/^{86}Sr$ values for the bulk and decarbonated beach ridge sample suggest that marine biogenic carbonates are a minor sediment component at the coast.

Our reassessment of the late 19th – early 20th century bathymetry with the high-resolution digital elevation model produced several surprises (Figs. 3 and 4a). First, the edge of the shelf (Fig. 4) was found to be significantly deeper in front of the Mottama Depression (>150 m) then west of it (100–120 m deep). Second, the mud belt along the Ayeyawady delta exhibits a typical clinoform profile attached to the coastline and extending to depths of 35–40 m. In contrast, the Gulf of Mottama exhibits a mid-shelf clinoform profile with the steep frontal region extending from 40 to 90 m water depth. The transition between the western and eastern clinoforms is marked by a transversal channel that is 10 km wide and 5 m deep on average and is flanked on the deeper eastern side by a drift-like elongated feature of similar average dimensions. Third, a flatter area of the outer shelf in front of the western Ayeyawady delta coast stands out from the typical outer shelf chaotic

relief, suggesting preservation of a relict pre-Holocene delta region at water depths between 35 and 45 m.

Discussion

Our new drill core information (Fig. 3) indicate that the Ayeyawady delta advanced into an incised valley estuarine embayment that extended north of Kyonmangay (~80 km from the current coast) but did not reach as far as the current delta apex at Ta Loke Htaw (270 km from the coast). The Pleistocene deposits of the incised valley intercepted in our cores are fluvial, generally much coarser than the delta deposits but heterolithic with indications of increasing tidal influence nearer to the Andaman Sea at Kyonmangay. The overlying peats atop mudflat sediments sampled at Kyonmangay indicate the presence of a muddy coast with mangroves at the time of their transgression ~9,300 years ago. Given that the contemporaneous ice-volume equivalent global sea level was between -29 and -31 mbsl (*Lambeck et al., 2014*), the altitude of the mangrove peat (-28.3 mbsl) on the largely incompressible Pleistocene deposits below indicate that the delta is vertically stable. After the mangrove coast was flooded, the marine embayment accumulated estuarine/prodelta muds afterwards. At 8,100 years ago the Ayeyawady bayhead delta front reached the southern Kyonmangay site and by ~6,300 years ago delta plain deposition started.

Deposits at the delta apex in the drill core at Ta Loke Htaw indicate a dynamic fluvial environment with a channel erosion event just before 1,300 years ago and point bar/floodplain deposition afterwards. This channel rejuvenation, in concert with luminescence dates constraining the activity and abandonment of the western Daga meander belt to not much after 1,500 years ago, suggest that the Ayeyawady partially or completely avulsed to the present eastern course close to that time. Meander belt construction on the old and new course of the river, leading to the formation of alluvial ridges, appears to be an efficient type of aggradation on the upper delta plain before the river starts to bifurcate. Although data is sparse to comment on possible connections, we note that this apparently major avulsion of the Ayeyawady took place during a period of intensified agricultural settlement and development of the Pyu city states in Central Myanmar (*Moore, 2007*), as well as a relatively wet interval in Southeast Asia (*Yamoah et al., 2016*), both conditions favoring higher discharges and sediment loads. Given the high seismicity of the region (*Wang et al., 2014*), large earthquakes (*Aung et al., 2008*) may have also played a role in the avulsion.

Near the coast, the quasi-contemporary beach ridge development on the Bogale Promontory and Yangon River mouth suggest that the advanced position of the western half of the delta was acquired early and maintained during progradation. Delta growth since 6,300 years ago, with intermediate stages delineated by successive beach ridge sets,

519 suggest decreasing rates of advance of ~25 m until ~4,600 years ago and 8 to 10 m
520 afterwards. The latter are still higher than the average progradation value of 3.4 m/year
521 calculated by *Hedley et al. (2010)* for the last century or so. Furthermore, the recent
522 progradation occurred primarily on the coast adjacent to both sides of the Yangon River,
523 while the shoreline of the rest of the delta has been largely immobile. It is important to
524 note that, like the Ayeyawady, many large river deltas developing under the Asian
525 monsoon regime, such as Mekong (*Ta et al., 2002*), Red River (*Tanabe et al., 2003*), or
526 Godavari (*Cui et al., 2017*) started to form wave-built beach ridges between 5000 and
527 4000 years ago changing from river-dominated morphologies to show stronger wave-
528 influenced characteristics. Given that these deltas were at various stages of advance from
529 within their incised valleys onto the shelf it is more likely that their morphological
530 evolution was climatically driven rather than controlled by local factors as previously
531 proposed. As the late Holocene monsoon aridification started at that time (*Ponton et al.,*
532 *2012*), fluvial discharge variability at centennial timescales increased setting the stage for
533 periodic wave-dominance of deltaic coasts during more arid intervals.
534
535 Our re-evaluation of the shelf morphology in the context of the new data onland reveals
536 important information for understanding the peculiar, irregular growth of the Ayeyawady
537 delta with its western half from Cape Maw Deng to the Bogale Promontory well
538 advanced into the Andaman Sea in comparison to its eastern half. First, the shelf DEM
539 suggests that the western Ayeyawady delta continues offshore into a shallow, shore-
540 attached clinoform, which is not completely unexpected given the relatively low tidal
541 range of 2–3 m (e.g., *Goodbred and Saito, 2012*) and the perennial loss of sediment
542 advected to the Gulf of Mottama (*Ramaswamy and Rao, 2014*). The Nd and Sr
543 fingerprint of the river sediment is almost identical to the beach ridge at Bogale
544 indicating that essentially no sediment from the Gulf of Mottama bearing the lower
545 radiogenic imprint of Sittaung or Thanlwin (*Damodararao et al., 2016*) is feeding this
546 part of the coast. The shore-attached clinoform tapers off after 40 mbsl (Fig. 2b). In
547 contrast, the Gulf of Mottama exhibits a mid-shelf clinoform with the roll-over at 40 m
548 and toe depth of 80–90 m. The internal architecture of this distinctive feature was imaged
549 previously (*Ramaswamy and Rao, 2014*) showing seismic characteristics typical of a
550 clinoform topset and foreset. Given the depressed character of the Mottama shelf
551 indicated by the shelf edge position 40 to 70 meter lower than in front of the western
552 Ayeyawady delta perhaps it is not surprising that infilling of this region is still ongoing.
553 What is surprising instead is why and how the Ayeyawady River built its delta on the
554 eastern raised shelf block rather than in advancing preferentially into the Gulf of
555 Mottama, defying theoretical and modeling expectations of a more advanced deltaic coast
556 toward the subsided block (e.g., *Liang et al., 2016*). The key to this problem appears to be
557 again suggested by the shelf morphology.
558

559 The distinctive transition between clinoforms exhibiting a wide elongated channel and
560 what appears to be an attached sediment drift-like feature suggests intense current activity
561 at the common clinoform boundary. Indeed tidal modeling suggests that a tidal shear
562 front (*Wang et al., 2017*) may be present in this region that shows a drastic change from
563 weak and isotropic tidal currents west of Bogale Promontory to highly oriented strong
564 currents in the Gulf of Mottama (*Rizal et al., 2012*). Such a shear front would explain
565 both the unusual channel-drift couplet, but also the fact the Ayeyawady was able to build
566 its delta west of the gulf. If the tidal shear front has been a long-lived feature of the shelf
567 circulation it probably acted as a littoral energy fence (*sensu Swift and Thorne, 1992*) that
568 helped trap a significant part of the Ayeyawady sediment on the raised western shelf
569 block. Given the depressed character of the Mottama shelf block, the front must have
570 existed since the beginning of the deglacial transgression of the northern Andaman shelf.
571 Industrial seismic reflection profiles imaged a region of strike-slip extension in the Gulf
572 of Mottama expressed as horsetail extensional splays linked to the Sagaing Fault system
573 (*Morley, 2017*) that can explain the height differential between the western and eastern
574 shelves. Furthermore, the shear front must have gradually intensified through positive
575 feedback with the morphology as the shore-attached clinoform west of it grew larger. In
576 contrast, the amplified tidal currents in the Gulf of Mottama efficiently redistributed the
577 significantly larger amount of Ayeyawady sediments that escaped beyond the energy
578 fence together with sediments from Sittaung and Thanlwin to form the midshelf
579 clinoform there. The offshore-directed tidal pumping leading to the formation of the
580 Mottama clinoform is reminiscent of the situation on the eastern Indus shelf where strong
581 tidal currents from the Gulf of Kutch built a mid-shelf clinoform with Indus sediments
582 escaping eastward (*Giosan et al., 2006*). Such clinoforms, which are of purely tidal
583 origin, and do not front a subaerial deltaic counterpart *per se* may have been more
584 common in sediment-rich macrotidal environments during faster transgressive conditions
585 in the past.
586
587 Conclusions
588
589 The Ayeyawady delta in Myanmar is the last realization in a long series of depocenters
590 that gradually moved southward within the tectonically dynamic intra-mountainous
591 landscape extending from the Central Myanmar Basin in the north to the northern
592 Andaman Sea in the south (Figs. 1 and 2). The delta appears to be be vertically stable
593 within the incised valley dug by the Ayeyawady River during the last lowstand (Fig. 3).
594 The Pleistocene valley was flooded at least 80 km inland from the present coast during
595 the deglacial sea level rise. Holocene progradation into this paleo-Ayeyawady bay
596 proceeded in the form of a fluvial- and tide-dominated delta until late Holocene wave
597 action began to build isolated and clustered beach ridges at the contemporaneous coasts
598 (Fig. 2). However, beach ridges are rather rare and underdeveloped, testifying to the

599 enormous sediment load discharged by the Ayeyawady and tidal dispersal and reworking.
600 Ridge construction during the late Holocene, similar to other several deltas across the
601 Indian monsoon domain, suggests a possible climatic control on delta morphodynamics
602 through variability in discharge, changes in wave climate, or both.
603
604 The landscape near the delta apex exhibits active and fossil late Holocene meander belts
605 that terminate in the mid-delta where the discharge is split to lower order distributary
606 channels (Fig. 2). The meander belts stand as alluvial ridges above the floodplain along
607 the active river course, as well as its antecedent paleo-course documenting the
608 Ayeyawady's avulsive character. Construction of a more advanced coast in the western
609 half of the delta could be seen as a quasi-independent region, the Pathein lobe (Fig. 5),
610 which was probably favored by the more western location of the early course of the river
611 (but see below). The eastern region of the delta (the Yangon lobe) is offset inland (Fig. 5)
612 and exhibits a more wave-dominated morphology, largely built with Ayeyawady-derived
613 sediment escaping alongshore. Further east, the Yangon lobe merges with the mudflats
614 fringing the Sittaung estuary (Fig. 5). Despite its large sediment load the Thanlwin River
615 has only built a bayhead delta, barely prograding outside its incised valley, probably due
616 to extreme macrotidal conditions at its mouth (Fig. 5). However, its sediment contributed
617 instead to deposition on the shelf, as did most of the load from both Ayeyawady and
618 Sittaung.
619
620 Correlation of the delta morphological and stratigraphic architecture information onland
621 to the shelf bathymetry and hydrodynamics, as well as its tectonic and sedimentary
622 characteristics, provides insight on the peculiar growth style of the Ayeyawady delta
623 (Figs. 2–5). The offset between the western Pathein lobe and the eastern deltaic coast
624 appears to be driven by tectonic-hydrodynamic feedbacks as the extensionally lowered
625 shelf block of the Gulf of Mottama amplifies tidal currents relative to the eastern part of
626 the shelf. This situation probably activates a perennial shear front between the two
627 regions that acts as a leaky energy fence helping to trap part of the sediment within the
628 Ayeyawady shore-attached subaqueous delta. Just as importantly, the strong currents in
629 the Gulf of Mottama act as an offshore-directed tidal pump that help build a deep, mixed-
630 source mid-shelf clinoform, the Ayeyawady-Sittaung-Thanlwin subaqueous delta, into
631 the Mottama shelf depression.
632
633 Our study takes a first look at the evolution of the Holocene Ayeyawady delta to provide
634 a basis for more detailed work and context to present and future management plans for
635 this ecologically and economically important, but vulnerable region. A first conclusion
636 for the future of the region comes by comparing the Ayeyawady to other deltas across the
637 world. Uniquely for deltas of its size the Ayeyawady delta has not suffered a sediment
638 deficit from damming, yet it has been barely growing. The reason is the highly energetic

Earth Surf. Dynam. Discuss., https://doi.org/10.5194/esurf-2017-64
Manuscript under review for journal Earth Surf. Dynam.
Discussion started: 20 November 2017

639 tidal, wind and wave regime of the northern Andaman Sea that export most sediments
640 offshore despite the large load of the river as envisioned by *Ramswamy et al., (2004)* and
641 *Hedley et al. (2010)*. In addition to their effects upstream (*Brakenridge et al., 2017*), the
642 expected sediment deficit after dams are constructed on the river and tributaries may
643 significantly impact the delta fragile sedimentary equilibrium (*Giosan et al., 2014*)
644 rendering it more vulnerable to the accelerating sea level rise (*Syvitski et al., 2009*) or
645 changes in frequency and intensity of cyclones hitting the coast (*Darby et al., 2016*).
646
647

Acknowledgments

This study was primarily supported by an Andrew W. Mellon Foundation Award for Innovative Research from the Woods Hole Oceanographic Institution to L. Giosan. We thank Myanmar authorities for project permissions as well as leaders and residents of villages that we visited in the Ayeyawady delta for hospitality and help. We also thank V. Ramaswamy (NIO, Goa) for providing inspiration with his previous Andaman Sea work and for help with initial contacts in Myanmar. N. Khonde gratefully acknowledges the SERB Indo-US Postdoctoral Fellowship sponsored by SERB-IUSSTF for research work at Woods Hole Oceanographic Institution, USA.

659 References
660

661 Aung, T.T., Satake, K., Okamura, Y., Shishikura, M., Swe, W., Saw, H., Swe, T.L., Tun,
662 S.T. and Aung, T., 2008. Geologic evidence for three great earthquakes in the past
663 3400 years off Myanmar. Journal of Earthquake and Tsunami, 2(04), pp.259-265.
664 Colarossi, D., Duller, G. A. T., Roberts, H. M., Tooth, S. & Lyons, R. 2015: Comparison
665 of paired quartz OSL and feldspar post-IR IRSL dose distributions in poorly bleached
666 fluvial sediments from South Africa. Quaternary Geochronology 30, 233-238.
667 Duller, G. A. T. 2003: Distinguishing quartz and feldspar in single grain luminescence
668 measurements. Radiation Measurements 37, 161–165.
669 Godfrey-Smith, D. L., Huntley, D. J. & Chen, W. H., 1988: Optically dating studies of
670 quartz and feldspar sediment extracts. Quaternary Science Reviews 7, 373–380.
671 Kars, R. H., Reimann, T., Ankjaergaard, C. & Wallinga, J. 2014: Bleaching of the post-
672 IR IRSL signal: new insights for feldspar luminescence dating. Boreas 43, 780–791.
673 Madsen, A.T., Buylaert, J.-P. & Murray, A.S. 2011. Luminescence dating of young
674 coastal deposits from New Zealand using feldspar. Geochronometria 38, 378-390.
675 Murray, A. S., Marten, R., Johnston, A. & Martin, P. 1987: Analysis for naturally
676 occurring radionuclides at environmental concentrations by gamma spectrometry.
677 Journal of Radioanalytical and Nuclear Chemistry 115, 263–288.
678 Murray, A. S. & Wintle, A. G. 2000: Luminescence dating of quartz using an improved
679 single-aliquot regenerative-dose protocol. Radiation Measurement 32, 57–73
680 Murray, A. S., Thomsen, K. J., Masuda, N., Buylaert, J.-P. & Jain, M. 2012: Identifying
681 well-bleached quartz using the different bleaching rates of quartz and feldspar
682 luminescence signals. Radiation Measurements 47, 688–695.
683 Rémillard, A.M., St-Onge, G., Bernatchez, P., Hétu, B., Buylaert, J.-P., Murray, A.S.,
684 Vigneault, B., 2016. Chronology and stratigraphy of the Magdalen Islands
685 archipelago from the last glaciation to the early Holocene: new insights into the
686 glacial and sea-level history of eastern Canada. Boreas, 45, 604-628.
687 Thomsen, K., Murray, A. S., Jain, M. & Bøtter-Jensen, L. 2008: Laboratory fading rates
688 of various luminescence signals from feldspar-rich sediment extracts. Radiation
689 Measurements 43, 1474–1486.
690 Adas, M.: The Burma Delta: Economic Development and Social Change on an Asian
691 Rice Frontier, 1852–1941, New Perspectives in SE Asian Studies, Univ of Wisconsin
692 Press, 276 pp., 2011.
693 Brakenridge, G. R., Syvitski, J. P. M., Nieburh, E., Overeem, I., Higgins, S. A., Kettner,
694 A. J. and Prades, L.:Design with nature: causation and avoidance of catastrophic
695 flooding, Myanmar. Earth-Science Rev. 165, 81–109, 2017.
696 British Admiralty: Bay of Bengal. East Coast. Sheet III. Coronge Island to White Point,
697 including the Gulf of Martaban, 1935.
698 Bronk Ramsey, C.: Bayesian analysis of radiocarbon dates. Radiocarbon, 51(1), 337-360,
699 2009.
700 Croudace, I. W. and Rothwell, R. G.: Micro-XRF Studies of Sediment Cores,
701 Developments in Paleoenvironmental Research, 17, Springer, 656 pp., 2015.
702 Croudace, I. W., Rindby, A. and Rothwell, R. G. ITRAX: description and evaluation of a
703 new X-ray core scanner. In New Techniques in Sediment Core Analysis (ed.
704 Rothwell, R. G.) Geol. Soc. Lond. Spec. Publ. 267, 51–63, 2006.

Cui, M, Wang, Zhanghua, Nageshwara Rao, Kakani, Sangode, S. J., Saito, Yoshiki, Ting, Chen, Kulkarni Y. R., Ganga Kumar, K. Ch. V., Demudu.: A mid-to-late Holocene record of vegetation decline and erosion triggered by monsoon weakening and human adaptations in the south–east Indian Peninsula; The Holocene, 0959683617715694, 2017.

Curray, J. R.: Tectonics of the Andaman Sea region: Journal of Asian Earth Sciences, v. 25, 187–232, doi: 10.1016 /j.jseaes .2004 .09 .001, 2005.

Curray, J. R., Moore, D. G., Lawver, L.A., Emmel, F.J., and Raitt, R.W.: Tectonics of the Andaman Sea and Myanmar, in Watkins, J., et al., eds., Geological and Geophysical Investigations of Continental Margins: American Association of Petroleum Geologists Memoir 29, 189–198, 1979.

Darby, S. E., Hackney, C. R., Leyland, J., Kummu, M., Lauri, H., Parsons, D. R., Best, J. L., Nicholas, A. P. and Aalto, R.: Fluvial sediment supply to a mega-delta reduced by shifting tropical-cyclone activity, Nature 539, (7628), 276-279, 2016.

D'Arrigo, R. and Ummenhofer, C. C.: The climate of Myanmar: evidence for effects of the Pacific Decadal Oscillation, Int. J. Climatol., 35, 634–640, doi:10.1002/joc.3995, 2014.

Damodararao K., Singh S. K, Rai V. K., Ramaswamy, V. and Rao, P. S.: Lithology, Monsoon and Sea-Surface Current Control on Provenance, Dispersal and Deposition of Sediments over the Andaman Continental Shelf. Front. Mar.Sci.3:118, 2016.

Farr, T. G., Rosen, P. A., Caro, E., Crippen, R., Duren, R., Hensley, S., Kobrick, M., Paller, M., Rodriguez, E., Roth, L. and Seal, D.: The Shuttle Radar Topography Mission. Rev Geophys 45: 10.1029/2005RG000183, 2007.

Fritz, H. M., Blount,C. D., Thwin, S., Thu, M. K. and Chan, N.: Cyclone Nargis storm surge in Myanmar. Nature Geoscience, 2, 448-449, 2009.

Furuichi, T., Win, Z., Wasson, R.J.: Discharge and suspended sediment transport in the Ayeyarwady River, Myanmar: centennial and decadal changes. Hydrol. Process. 23 (11), 1631–1641, 2009.

Garzanti, E.,Wang, J. G., Vezzoli, G. and Limonta, M.: Tracing provenance and sediment fluxes in the Irrawaddy River basin (Myanmar). Chemical Geology, 440, 73–90, 2016.

Gebregiorgis, D., Hathorne, E. C., Sijinkumar, A. V., Nagender Nath, B., Nürnberg, D. and Frank, M.: South Asian summer monsoon variability during the last ~54 kyrs inferred from surface water salinity and river run off proxies, Quaternary Science Reviews 138: 6-15, 2016.

Giosan, L., Ponton, C., Usman, M., Blusztajn, J., Fuller, D., Galy, V., Haghipour, N., Johnson, J., McIntyre, C., Wacker, L. and Eglinton, T.: Massive Erosion in Monsoonal Central India Linked to Late Holocene Landcover Degradation, Earth Surface Dynamics, in review, 2017.

Giosan, L., Constantinescu, S., Clift, P. D., Tabrez, A. R., Danish, M. and Inam, A.: Recent morphodynamics of the Indus delta shore and shelf. Continental Shelf Research, 26(14),1668-1684, 2006.

Giosan, L., Syvitski, J. P. M., Constantinescu, S., Day, J.: Protect the World's Deltas, Nature, 516: 31-33, 2014.

749 Goodbred S. L. and Saito, Y.: Tide dominated deltas. In Principles of Tidal
750 Sedimentology, ed. RA Davis Jr, RW Dalrymple, pp. 129–49. London: Springer,
751 2012.
752 Gordon, R.: Hydraulic work in the Irawadi Delta. Proc. Inst. Civ. Eng. 113 (1893), 276–
753 313, 1893.
754 Hedley, P. J., Bird, M. I. and Robinson, R. A. J.: Evolution of the Irrawaddy delta region
755 since 1850. Geogr. J. 176 (2), 138–149, 2010.
756 Hoitink, A. J. F., Wang, Z. B., Vermeulen, B., Huismans, Y. and Kästner, K.: Tidal
757 controls on river delta morphology. Nature Geoscience, 10(9), 637-645, 2017.
758 Kravtsova, V. I., Mikhailov, V. N. and Kidyaeva, V. M.: Hydrological regime,
759 morphological features and natural territorial complexes of the Irrawaddy River Delta
760 (Myanma r). Vodn. Resur. 36, 259–276, 2009.
761 Liang, M., Kim, W. and Passalacqua, P.: How much subsidence is enough to change the
762 morphology of river deltas?. Geophysical Research Letters, 43(19), 2016.
763 Matamin, A. R., Ahmad, F., Mamat, M., Abdullah, K. and Harun, S.: Remote sensing of
764 suspended sediment over Gulf of Martaban. Ekologia, 34(1), 54-64, 2015.
765 McHugh, M. G. C., Gurung, D., Giosan, L., Ryan, W.B.F., Mart, Y., Sancar, U., Burckle,
766 L., Çagatay, M. N.: The last reconnection of the Marmara Sea (Turkey) to the World
767 Ocean: A paleoceanographic and paleoclimatic perspective, Marine Geology, 255,
768 2008.
769 Milliman, J. D. and Farnsworth, K. L.: River Discharge to the Coastal Ocean: A Global
770 Synthesis. Cambridge Univ. Press, Cambridge, 2010.
771 Moore E. H.:, Early Landscapes of Myanmar, River Books, Bangkok , pp., 272, 2007.
772 Morley, C.K. 2017. Cenozoic rifting, passive margin development and strike-slip faulting
773 in the Andaman Sea: a discussion of established v. new tectonic models. In:
774 Bandopadhyay, P.C. & Carter, A. (eds) The Andaman–Nicobar Accretionary Ridge:
775 Geology, Tectonics and Hazards. Geological Society, London, Memoirs, 47, 27–50,
776 https://doi.org/10.1144/M47.4
777 Ota, Y., Kawahata, H., Murayama, M., Inoue, M., Yokoyama, Y., Miyairi, Y., Aung, T.,
778 Hossain, H. M. Z., Suzuki, A., Kitamura, A., Moe, K. T.: Effects of intensification of
779 the Indian Summer Monsoon on northern Andaman Sea sediments during the past
780 700 years. J. Quat. Sci. 32, 528–539, 2017.
781 Ponton, C., Giosan, L., Eglinton, T. I., Fuller, D. J., Johnson, E., Kumar, P. and Collet, T.
782 S.: Holocene Aridification of India. Geophysical Research Letters, 39, p. L03704,
783 2012.
784 Racey, A. and Ridd, M.F.: Petroleum Geology of Myanmar. Geological Society of
785 London, 2015.
786 Ramaswamy V., Rao P. S., Rao K. H., Thwin, S., Rao, Srinivasa N. and Raiker, V.: Tidal
787 influence on suspended sediment distribution and dispersal in the northern Andaman
788 Sea and Gulf of Martaban Marine Geology 208 33–42, 2004.
789 Ramaswamy, V., and Rao, P. S.The Myanmar continental shelf. In F. L. Chiocci & A. R.
790 Chivas (Eds.), Continental Shelves of the World: Their Evolution During the Last
791 Glacio-Eustatic Cycle (pp. 231-240). Bath, UK: Geological Society of London, 2014.
792 Rao, P. S., Ramaswamy, V. and Thwin, S.: Sediment texture, distribution and transport
793 on the Ayeyarwady continental shelf, Andaman Sea. Mar. Geol. 216, 239–247 2005.

Reimer P. J., Bard, E., Bayliss, A., Beck, J. W., Blackwell, P. G., Bronk, Ramsey C, Buck, C. E., Edwards, R. L., Friedrich, M., Grootes, P. M., Guilderson, T. P., Haflidason, H., Hajdas, I., Hatté, C., Heaton, T. J., Hoffman, D. L., Hogg, A. G., Hughen, K. A., Kaiser, K. F., Kromer, B., Manning, S. W., Niu, M., Reimer, R. W., Richards, D. A., Scott, M., Southon, J. R., Staff, R. A., Turney, C. S,. M., van der Plicht, J.: IntCal13 and Marine13 radiocarbon age calibration curves 0–50,000 years cal BP. Radiocarbon 55(2): 1869-1887, 2013.

Rizal, S., Damm, P., Wahid, M.A., Sundermann, J., Ilhamsyah, Y. and Iskandar T.: General circulation in the Malacca Strait and Andaman Sea: A numerical model study. American Journal of Environmental Sciences. 8. 479-488. 10.3844/ajessp.2012.479.488. , 2012.

Robinson, R. A. J., Bird, M. I., Oo, N. W., Hoey, T. B., Aye, M.M., Higgitt, D. L., Swe, A., Tun, T. and Win, S.L.: The Irrawaddy river sediment flux to the Indian Ocean: the original nineteenth-century data revisited. The Journal of Geology, 115(6), 629-640, 2007.

Rodolfo KS. 1975. The Irrawaddy Delta: Tertiary setting and modern offshore sedimentation. In Deltas: Models for Exploration, Broussard ML (ed.). Houston Geological Society: Houston; 329–348.

Rodolfo K S 1969a Bathymetry and marine geology of the Andaman Basin, and tectonic implications for Southeast Asia Geological Society of America Bulletin 80 1203–30

Rodolfo, K. S.: Sediments of the Andaman Basin, Northeastern Indian Ocean. Mar. Geol. 7, 371– 402, 1969b.

Scher H. D. and M. L.: Delaney, Braking the glass ceiling for high resolution Nd records in early Cenozoic paleoceanography.Chemical Geology 269, 269-329, 2010..

Seekins, D. M.: "State, society and natural disaster: cyclone Nargis in Myanmar (Burma)", Asian Journal of Social Science, 37(05), pp.717-37, 2009.

Shi,W. and Wang, M.: Three-dimensional observations from MODIS and CALIPSO for ocean responses to cyclone Nargis in the Gulf of Martaban. Geophysical Research Letters, 35, L21603, 2008.

Stamp, D. L. The Irrawaddy River. Geogr. J. 5, 329–352, (1940).

Swift, D. J. P. and Thorne, J. A.: Sedimentation on Continental Margins, I: A General Model for Shelf Sedimentation, in Shelf Sand and Sandstone Bodies: Geometry, Facies and Sequence Stratigraphy (eds D. J. P. Swift, G. F. Oertel, R. W. Tillman and J. A. Thorne), Blackwell Publishing Ltd., Oxford, UK. doi: 10.1002/9781444303933.ch1, 1992.

Syvitski, J. P., Kettner, A. J., Overeem, I., Hutton, E.W., Hannon, M.T., Brakenridge, G.R., Day, J., Vörösmarty, C., Saito, Y., Giosan, L. and Nicholls, R.J., Sinking deltas due to human activities. Nature Geoscience, 2(10), 681-686, 2009.

Ta, T. K. O., Nguyen, V. L., Tateishi, M., Kobayashi, I., Saito, Y. and Nakamura, T.,. Sediment facies and Late Holocene progradation of the Mekong River Delta in Bentre Province, southern Vietnam: an example of evolution from a tide-dominated to a tide- and wave-dominated delta. Sedimentary Geology, 152(3), 313-325, 2002.

Taft, L. and Evers, M.: A review of current and possible future human-water dynamics in Myanmar's river basins. Hydrological Earth System Science 20: 4913-4928, 2016.

838 Tanabe, S., Hori, K., Saito, Y., Haruyama, S. and Kitamura, A.: Song Hong (Red River)
839 delta evolution related to millennium-scale Holocene sea-level changes. Quaternary
840 Science Reviews, 22(21), 2345-2361, 2003.
841 Volker, A.: The deltaic area of the Irrawaddy river in Burma in Scientific problems of the
842 humid tropical zone deltas and their implications Proceedings of the Dacca
843 Symposium UNESCO 373–9, 1966.
844 Wang, Y., Sieh, K., Tun, S.T., Lai, K.Y. and Myint, T., 2014. Active tectonics and
845 earthquake potential of the Myanmar region. Journal of Geophysical Research: Solid
846 Earth, 119(4), pp.3767-3822.
847 Wang, N., Li, G., Qiao, L., Shi, J., Dong, P., Xu, J. and Ma, Y.: Long-term evolution in
848 the location, propagation, and magnitude of the tidal shear front off the Yellow River
849 Mouth. Continental Shelf Research, 137, 1-12, 2017.
850 Yamoah, K. A., Higham, C. F., Wohlfarth, B., Chabangborn, A., Chawchai, S., Schenk,
851 F. and Smittenberg, R. H.:Societal response to monsoonal fluctuations in NE
852 Thailand during the demise of Angkor Civilisation. The Holocene,
853 p.0959683617693900, 2017.
854

Earth Surf. Dynam. Discuss., https://doi.org/10.5194/esurf-2017-64
Manuscript under review for journal Earth Surf. Dynam.
Discussion started: 20 November 2017

Table 1. Results of AMS ^{14}C dating of organic materials from drill cores IR1 (Kyonmangay) and IR2 (Ta Loke Htaw).

Location	Sample	Altitude (*m bsl*)	Type	Labcode	Latitude	Longitude	Age (*years BP*)	Error (*years BP*)	d13C (*per mil*)	Calibrated Age (*years*)*	Error (*years*)	Observations
Kyonmangay	IR1-9.60	-2.9	leaf fragment	OS-132754	16°26'15N	95°08'01"E	5,590	100	-28.65	6487	213	small
Kyonmangay	IR1-20.0	-13.3	leaf fragment	OS-132658	16°26'15N	95°08'01"E	7,300	40	-26.71	8166	80	
Kyonmangay	IR1-35.0	-28.3	mangrove wood piece	OS-133490	16°26'15N	95°08'01"E	8,300	40	-27.27	9352	148	
Kyonmangay	IR1-40.0	-33.3	carbonized wood piece	OS-132659	16°26'15N	95°08'01"E	9,100	35	-26.58	10351	88.5	
Ta Loke Htaw	IR2-19.0	-0.5	wood trunk piece	OS-133606	17°39'13"N	95°26'2"E	1,320	15	-28.04	1307	53.5	
Ta Loke Htaw	IR2-33.5	-15.0	carbonized wood piece	OS-135132	17°39'13"N	95°26'2"E	8,020	30	-27.7	8959	117.5	small

*Calendar ages are relative to year 2016

Earth Surf. Dynam. Discuss., https://doi.org/10.5194/esurf-2017-64
Manuscript under review for journal Earth Surf. Dynam.
Discussion started: 20 November 2017

Table 2. Summary of the quartz and feldspar luminescence data. (n) denotes the number of aliquots contributing to dose (De). The saturated water content (w.c.) is given as the ratio of weight of water to dry sediment weight. Feldspar IR50 and pIRIR150 ages have not been corrected for any signal instability. Radionuclide concentrations used to derive quartz and feldspar dose rates are given in Table S1. Bleaching of quartz OSL signal is assessed by comparing the quartz ages with the IR50 and pIRIR150 ages. Uncertainties represent one standard error. Age uncertainties include random and systematic components. Quartz ages should be used for interpretation; feldspar ages are only used to investigate quartz OSL bleaching.

Sample code	Site	Setting	Latitude / Longitude	Depth, cm	Quartz well-bleached?	Quartz Age , ka	$pIRIR_{150}$ Age , ka	IR_{50} Age , ka	Quartz Dose , Gy (n)	$pIRIR_{150}$ Dose , Gy	IR_{50} Dose , Gy (n)	Quartz Dose rate, Gy/ka	K-feldspar Dose rate, Gy/ka	w.c. %
17 72 01	I8	fluvial levee	N 17 38 36.82 / E 95 18 33.64	95	probably	**1.50 ± 0.23**	6.64 ± 0.68	1.20 ± 0.23	**3.28 ± 0.49 34**	20.6 ± 1.9	3.73 ± 0.69 9	**2.19 ± 0.10**	3.10 ± 0.12	**29**
17 72 02	I9	fluvial levee	N 17 36 13.5 / E 95 12 53.39	110	not certain	**1.75 ± 0.32**	15.2 ± 5.5	4.02 ± 1.85	**4.14 ± 0.73 35**	46 ± 16	12.0 ± 5.5 9	**2.37 ± 0.10**	2.99 ± 0.11	**35**
17 72 03	I10	beach ridge	N 16 09 03.5 / E 94 43 57.3	92	probably	**1.46 ± 0.22**	2.35 ± 0.21	1.10 ± 0.07	**2.97 ± 0.42 40**	6.9 ± 0.5	3.25 ± 0.17 9	**2.03 ± 0.09**	2.95 ± 0.11	**28**
17 72 04	I11	beach ridge	N 16 09.2578 / E 94 44.1843	90	confident	**4.63 ± 0.47**	4.73 ± 0.37	2.71 ± 0.17	**10.1 ± 0.9 36**	14.7 ± 1.0	8.42 ± 0.43 9	**2.18 ± 0.09**	3.10 ± 0.11	**32**
17 72 05	I12	beach ridge	N 15 50 10.5 / E 95 29 51	100	probably	**1.04 ± 0.09**	1.94 ± 0.19	0.79 ± 0.05	**2.64 ± 0.17 38**	6.7 ± 0.6	2.72 ± 0.14 9	**2.53 ± 0.13**	3.45 ± 0.15	**38**
17 72 06	I13	beach ridge	N 15 49.6494 / E 95 30.2095	132	probably	**0.86 ± 0.07**	1.86 ± 0.15	0.68 ± 0.04	**1.58 ± 0.12 37**	5.1 ± 0.4	1.88 ± 0.08 9	**1.84 ± 0.07**	2.75 ± 0.10	**40**
17 72 07	I14	beach ridge	N 16 24 27.5 / E 96 02 20.2	115	probably	**1.19 ± 0.11**	1.43 ± 0.12	0.76 ± 0.04	**2.64 ± 0.19 40**	4.5 ± 0.3	2.38 ± 0.09 9	**2.21 ± 0.10**	3.13 ± 0.12	**24**

Earth Surf. Dynam. Discuss., https://doi.org/10.5194/esurf-2017-64
Manuscript under review for journal Earth Surf. Dynam.
Discussion started: 20 November 2017

869 Fig. 1. Physiography (left) and geology (right) of the Ayeyawady Basin and adjacent regions.
870

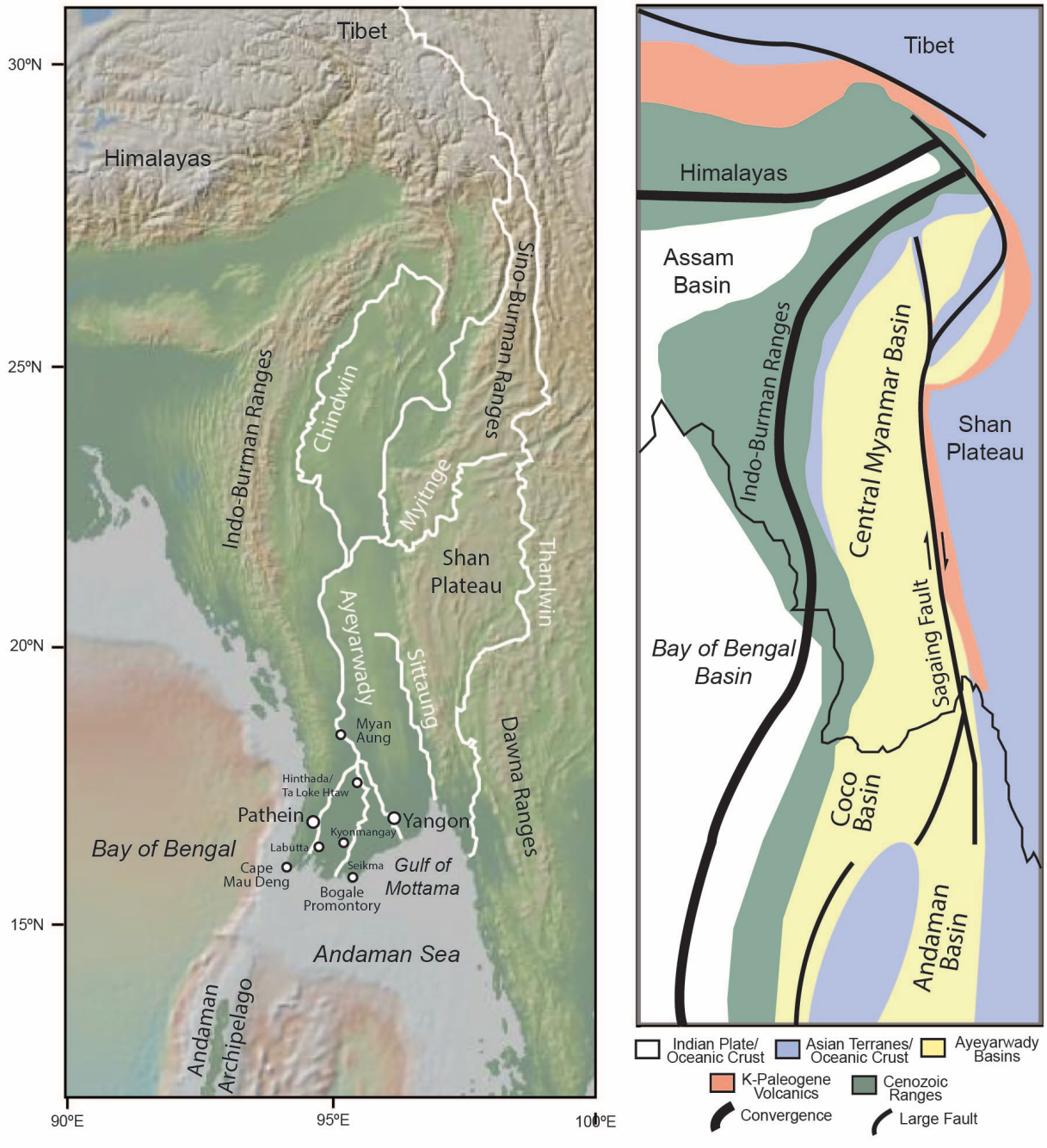

Earth Surf. Dynam. Discuss., https://doi.org/10.5194/esurf-2017-64
Manuscript under review for journal Earth Surf. Dynam.
Discussion started: 20 November 2017

Fig. 2. (a) SRTM-derived DEM for the Ayeyawady delta region (pattern of colors repeats every 10 m to 300 m in height; higher landscape in black); (b) large scale features of the Ayeyawady delta region with identified river and distributary courses and mouths as well as beach ridges shown on an ASTER satellite photo ; (c) sample locations and chronology on the meander belts documenting the avulsion near the delta apex (meander belts as white lines delimited from ASTER and Google Earth images); (d) Preliminary model of the Ayeyawady delta evolution with sampling locations and types with chronological information on the youngest fluvial deposits and beach ridges.

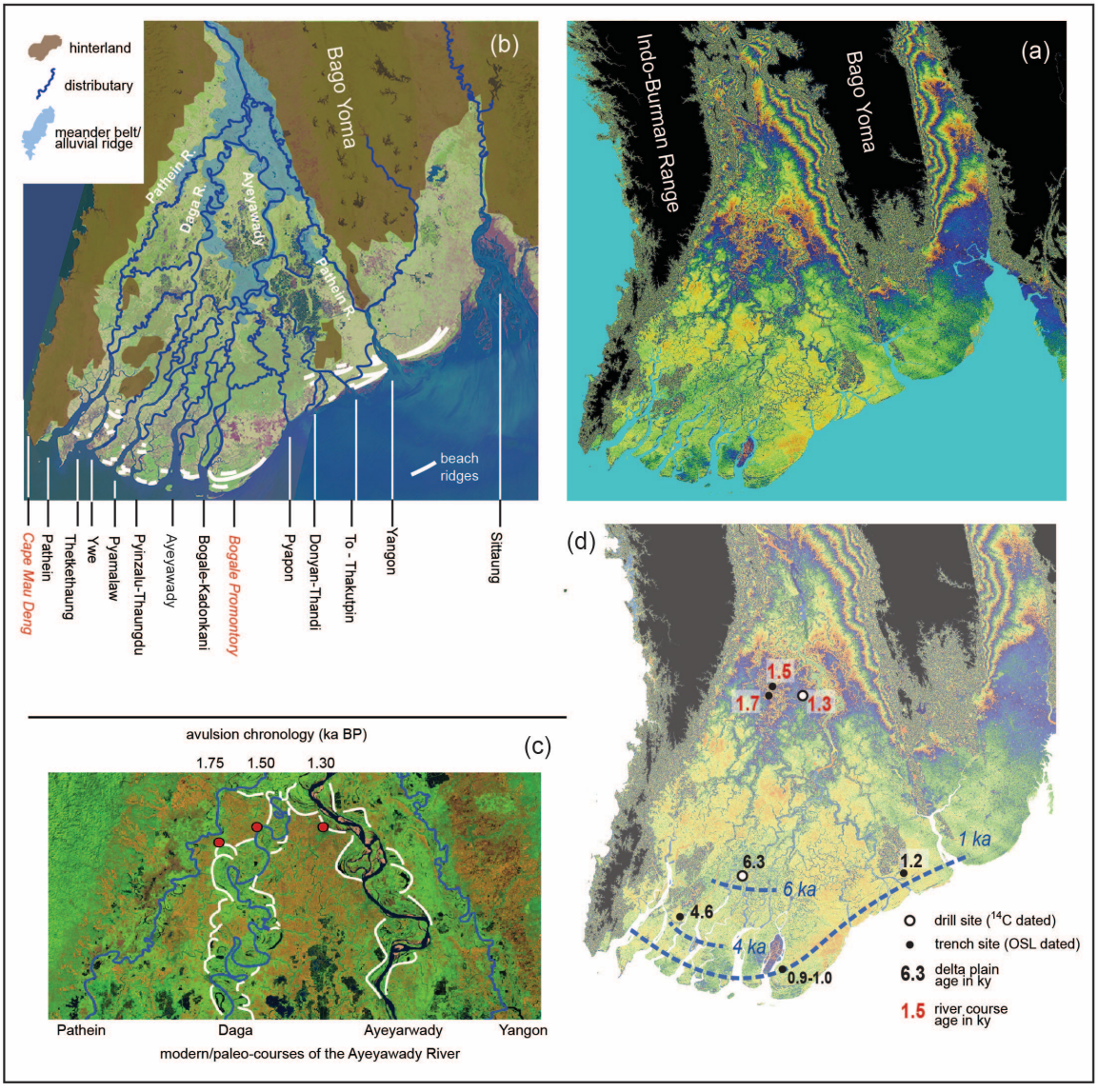

Earth Surf. Dynam. Discuss., https://doi.org/10.5194/esurf-2017-64
Manuscript under review for journal Earth Surf. Dynam.
Discussion started: 20 November 2017

882 Fig. 3. (a) Depositional environments interpreted from litho- and chemo-stratigraphy with
883 radiocarbon chronology for drill cores in the Ayeyawady delta; (b) Interpreted Ayeyawady
884 delta stratigraphy and evolution along the Ayeyawady's main course.

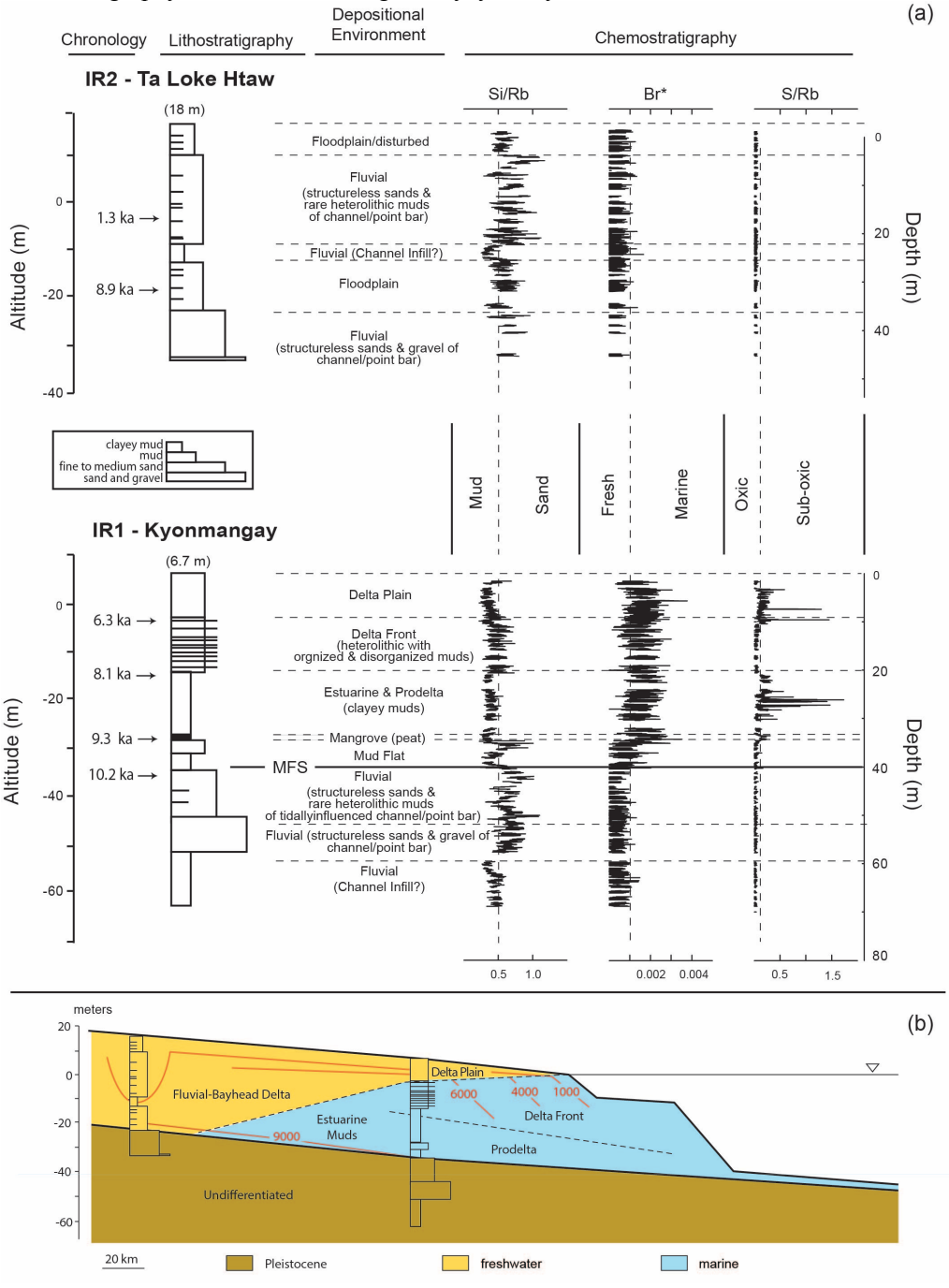

885

Earth Surf. Dynam. Discuss., https://doi.org/10.5194/esurf-2017-64
Manuscript under review for journal Earth Surf. Dynam.
Discussion started: 20 November 2017

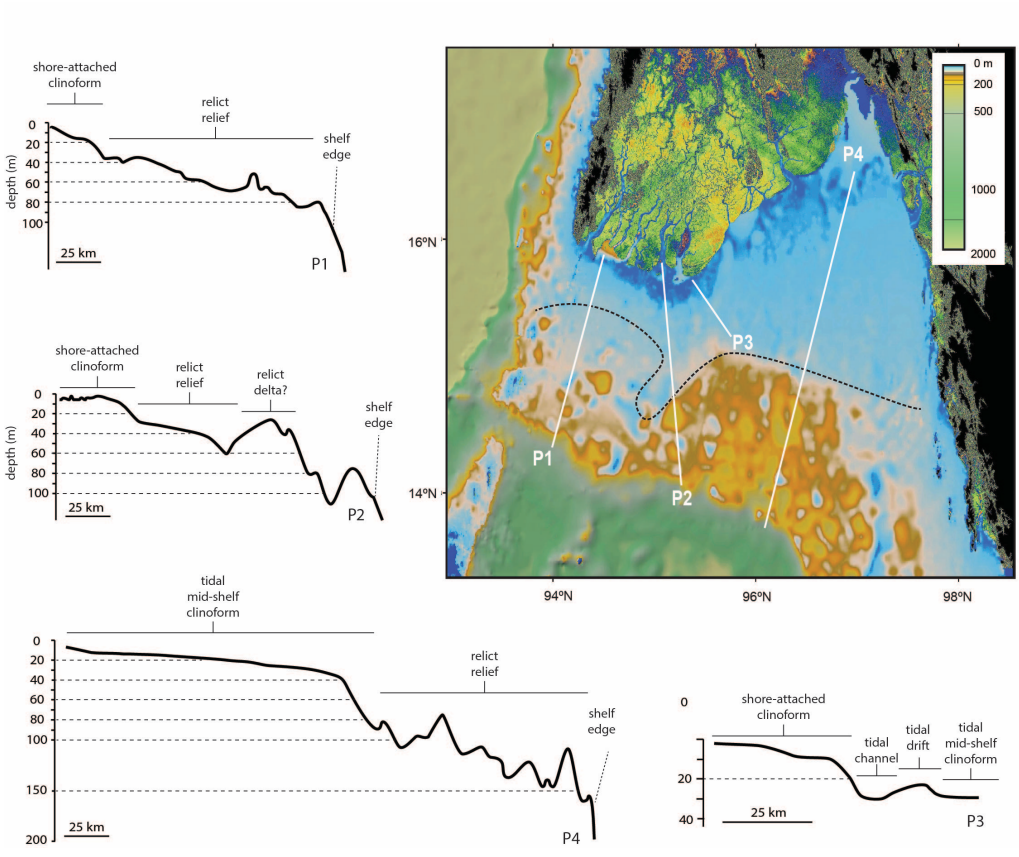

Fig. 4. Interpreted bathymetric profiles across the northern Andaman Sea shelf (bathymetric profiles identified on map). Dashed line on map indicates the approximate limit of consistent fine-grained sediment deposition on the shelf farthest from shore. The SRTM-derived DEM for the Ayeyawady delta region is shown onland.

Earth Surf. Dynam. Discuss., https://doi.org/10.5194/esurf-2017-64
Manuscript under review for journal Earth Surf. Dynam.
Discussion started: 20 November 2017

909 Fig. 5. (Upper) Bathymetry of the northern Andaman Sea shelf and SRTM-derived DEM for
910 the Ayeyawady delta region onland with regional faults and associated splay faults (Morley,
911 2017); (Middle) Tidal range lines (black), co-tidal lines (white) and tidal current magnitudes
912 (ellipses) for the dominant M2 tide component (Rizal et al., 2012); (Lower) Sketch he
913 Ayeyawady delta plain evolution phases and associated subaqueous deltas.

Earth Surf. Dynam. Discuss., https://doi.org/10.5194/esurf-2017-64
Manuscript under review for journal Earth Surf. Dynam.
Discussion started: 20 November 2017